CHEMISTRY
A EUROPEAN JOURNAL

DOI: 10.1002/chem.200902490

# Molecular Template Assisted Growth of Ultrathin Silicon Carbide Nanowires with Strong Green Light Emission and Excellent Field-Emission Properties

**Guangcheng Xi,*[a] Yanting He,[b] and Chao Wang[b]**

**Abstract:** A novel molecule template assisted chemical co-reduction method has been successfully developed for the controlled synthesis of ultrathin β-SiC single-crystalline nanowires on a large scale. The ultrathin β-SiC single-crystalline nanowires are about 8 nm in diameter and 200–800 nm in length. The resulting thin β-SiC single-crystalline nanowire is new in the family of β-SiC one-dimensional (1D) nanostructures. A synergistic action of π-stacking and steric hindrance result from the 1,10-phenanthroline molecule template are proposed to explain the growth mechanism of the ultrathin β-SiC single-crystalline nanowires based on the experimental observation. Importantly, such ultrathin β-SiC nanowire has shown a strong structure-induced enhancement of photoluminescence properties and has exhibited a very strong green light emission, which can be seen by naked eye. Furthermore, the unique β-SiC ultrathin nanowire structure exhibits a low turn-on field ($3.57\ V\,\mu m^{-1}$) and a large field-emission current density ($20\ mA\,cm^{-2}$). These results suggest that the ultrathin β-SiC nanowires can be expected to find promising applications as field emitters and photoelectronic devices.

**Keywords:** field emission · luminescence · nanostructures · silicon carbides · template synthesis

## Introduction

It is generally recognized nowadays that nanowires provide a good platform for investigate the dependence of the electrical and thermal transport or mechanical properties on dimensionality.[1–4] They are also received considerable attention due to their potential use in fabricating new type of electronic, optoelectronic, magnetic, and electromechanical nanodevices.[5–7] Nanowire-based applications demand nanowires with controlled diameter, length, morphology, and composition. Various strategies have been adopted to control the growth of nanowires, including surfactants, DNA, and polymers induced growth (so-called soft-template methods),[8–10] vapor–liquid–solid (VLS) and solution–liquid–solid (SLS) phase catalytic growth,[11–13] oriented attachment of nanoparticles,[14–17] and templated growth inside nanopores.[18–19] Although good control over nanowires diameter and length has been realized via these strategies, the developement of simple and effective techniques that can be used to control the size and shape of the nanowires prepared under high-temperature conditions remains a big challenge. For example, the size- and shape-controlled syntheses of metal and semiconductor nanowires have been achieved in low-temperature solution phase routes by employing appropriate soft templates,[8–10] however, most of the templates will be pyrolyzed and carbonized when reaction temperature is above 500 °C. Therefore, the soft-template methods are not fitted for size- and shape-controlled synthesis of nanowires in high temperature synthetic routes, such as vapor–liquid–solid (VLS)[11–13] and vapor–solid (VS) routes.[20–21] On the other hand, it is very difficult to synthesize certain materials, which have a high crystallization energy barrier (such as SiC and $Si_3N_4$) via low-temperature solution-phase method.[22] Although hard templates such as porous aluminum oxide have been successfully used to fabricate nanowires in high temperature conditions,[23] removal of hard templates from the nanowires surface can require harsh conditions. Therefore, it is very important to develop new methods that can be used in shape- and size-controlled high-temperature synthetic route.

[a] Dr. G. Xi
International Center for Materials Nanoarchitectonic and Photocatalytic Materials Center
National Institute for Materials Science
1-2-1 Sengen, Tsukuba, Ibaraki 305-0047 (Japan)
Fax: (+81) 29-859-2601
E-mail: Xi.guangcheng@nims.go.jp

[b] Dr. Y. He, Prof. C. Wang
Inspection and Research Center for Nanomaterials and Nanoproducts
Chinese Academy of Inspection and Quarantine
Beijing 100123 (P. R. China)

Cubic zinc blende (CZB) silicon carbide (β-SiC), as an important Group IV–IV semiconductor ($E_g = 2.39$ eV at room temperature), has extreme hardness and high thermal conductivity even at high temperature.[24] Recently, β-SiC nanowire structure attracts much attention owing to their potential applications based on field electron emission, catalysis, and ceramic properties.[25–28] Several high-temperature synthetic methods have been developed to synthesize high-quality β-SiC nanowires, such as thermal evaporation, arc-discharge, and chemical vapor deposition.[29–34] However, most of these β-SiC nanowires are synthesized by these high temperature routes process with relative larger diameters (generally larger than 20 nm). Shape- and size-controlled synthesis of β-SiC nanowires thus remains a great challenge. In particular, the large-scale synthesis of ultrathin β-SiC single-crystalline nanowires with diameter smaller than 10 nm and high aspect ratio has not been achieved, which greatly limits their applications.

In this paper, we report for the first time the synthesis, photoluminescence, and field-emission properties of a novel ultrathin β-SiC single-crystalline nanowire via a 1,10-phenanthroline-assisted molecule template route. The ultrathin β-SiC nanowires are single-crystalline and have an average diameter of 8 nm. In the present synthetic route, metal Mg is used as a mild reductant, and 1,10-phenanthroline is used as an effective molecule template for the formation of the ultrathin β-SiC nanowire structure. The molecule template route provides a novel strategy to synthesize ultrathin nanowires at relative higher temperature. Meanwhile, as a practical application, the obtained ultrathin β-SiC single-crystalline nanowires exhibit a strong green light emission, which can be seen by naked eye. Furthermore, this unique ultrathin β-SiC single-crystalline nanowire structure exhibits a low turn-on field ($3.57\ V\,\mu m^{-1}$), and a large field-emission current density ($20\ mA\,cm^{-2}$). These results suggest that the ultrathin β-SiC nanowires can be expected to find promising applications as field emitters and photoelectronic devices.

## Results and Discussion

Figure 1 shows the typical power X-ray diffraction (XRD) pattern of the as-synthesized product. All the peaks can be indexed as β-SiC with lattice constant of $a = 4.351$ Å, which is close to the value of β-SiC ($a = 4.359$ Å) (JCPDS, NO. 29-1129). No other crystalline impurities were detected by XRD, which indicates the pure β-SiC sample was obtained via the present synthetic route.

The morphology of the β-SiC nanowires were investigated by field-emission scanning electron microscopy (FESEM). Figure 2a shows the overall morphology of the sample, which indicates that the obtained product consists of large quantities of wire-like nanostructures. The nanowires are about 200–800 nm in length. The nanowires were further characterized by transmission electron microscopy (TEM). Figure 2b shows a typical TEM image of the ultrathin nanowires, showing that the nanowires are about 8 nm in diameter. Figure 2c shows an enlarged TEM image of one single nanowire, revealing that the surface of the nanowire is very smooth and clean. The inset is the corresponding selected area electron diffraction (SAED) pattern of the nanowire, which is consistent with that of β-SiC. The wire axis is parallel to the [111] direction of the cubic unit cell. High-resolution TEM (HRTEM) image of one single nanowire (Figure 2d) shows the (111) fringes are on average separated by 2.52 Å, which is about the same value as for bulk β-SiC, 2.5166 Å (JCPDS Card No. 29-1129). In addition, no silicon dioxide lays are found on the edge of the ultrathin β-SiC nanowires. Energy dispersive X-ray spectroscopy (EDS) characterization demonstrated that the wire-like structures are composed of silicon and carbon (Figure 2e). Silicon and carbon peaks can be clearly observed in this spectrum. The O and Cu peaks in the EDS spectrum arise from the ad-

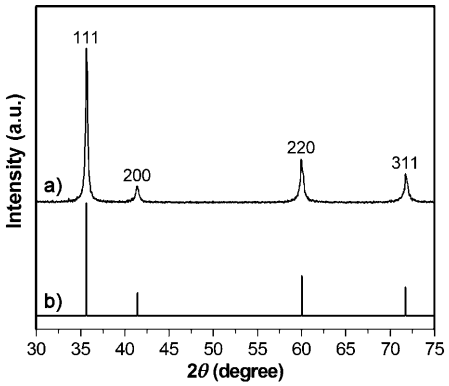


Figure 1. a) XRD pattern of the as-synthesized ultrathin β-SiC nanowires. b) Standard XRD pattern of β-SiC (JCPDS, No. 29-1129).

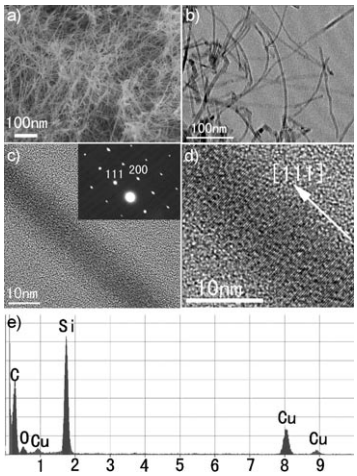


Figure 2. a) SEM image of the ultrathin β-SiC nanowires. b) Low-magnification TEM image of the ultrathin β-SiC nanowires. c) High-magnification TEM image of one single ultrathin β-SiC nanowire, the insert is the corresponding SAED pattern. d) HRTEM image of one single HRTEM image of one single ultrathin β-SiC nanowires. e) EDS spectrum of the ultrathin β-SiC nanowires.

  

sorbed oxygen and the copper TEM grid used in the measurements. Based on these characterization results, it can be rationally concluded that the ultrathin β-SiC single-crystalline nanowires are high crystalline and grows along the [111] direction.

The composition of the as-prepared nanowires was further analyzed by X-ray photoelectron spectra (XPS) (Figure 3). Figure 3a shows a typical survey spectrum of the ultrathin β-SiC nanowires, indicating the presence of elemental Si and C. The appearance of other peaks is due to the absorption of $CO_2$ and $O_2$ impurities on the surface of the sample. The binding energies centered at 100.5 eV for $Si_{2p}$ (Figure 3b) and 282.8 eV for $C_{1s}$ (Figure 3c) are in good agreement with the values of β-SiC. Quantification of the $Si_{2p}$ and $C_{1s}$ peaks gives an average Si/C atomic ratio of 0.97:1, which is close to the calculated atomic ratio, within the range of experimental error. The other two peaks at 281.1 and 286.9 eV in Figure 3c correspond to the absorbed small quantity of carbon and some organic molecules containing carbonyl functional groups.

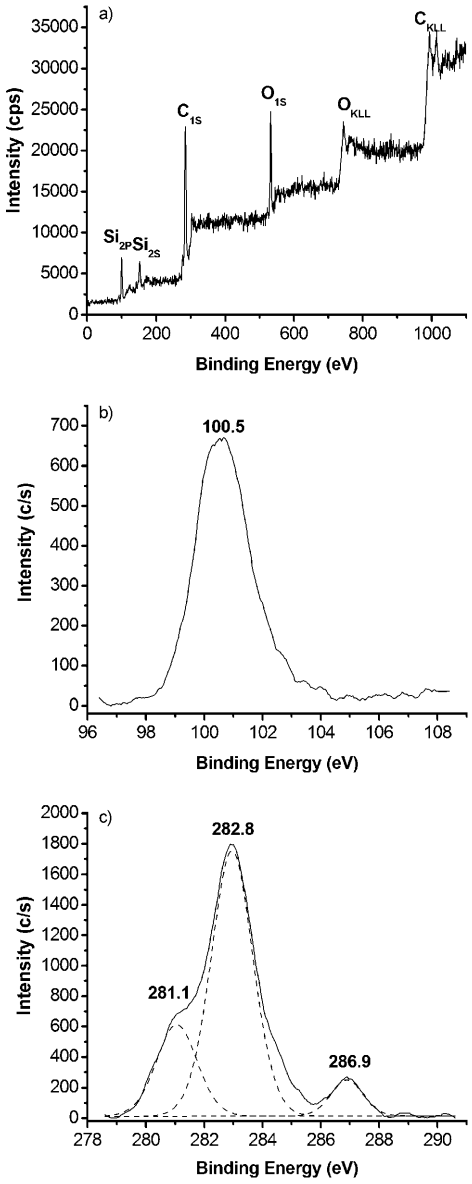


Figure 3. XPS spectra of the ultrathin β-SiC nanowires; a) survey spectrum; b) Si2p region; c) C1S region.

The Raman spectrum of as-synthesized ultrathin β-SiC nanowires (Figure 4a) shows the presence of one sharp peak at 793.8 $cm^{-1}$ and one weak peak at about 974.4 $cm^{-1}$, which correspond to the TO and LO phonons at the Γ point of β-SiC, respectively. The low intensity peaks marked with SF in the Raman spectra might be attributed to stacking faults in the nanowires. The Fourier transform infrared (FTIR) spectrum for the ultrathin β-SiC nanowires is shown in Figure 4b. The obvious absorption peak at about 814 $cm^{-1}$ can be indexed as the TO phonons of β-SiC, which is consistent with the early reports.[35] The bands at 3494 and 1628 $cm^{-1}$ are the stretching of O–H and flexural vibrations of the O–H in free water, respectively.

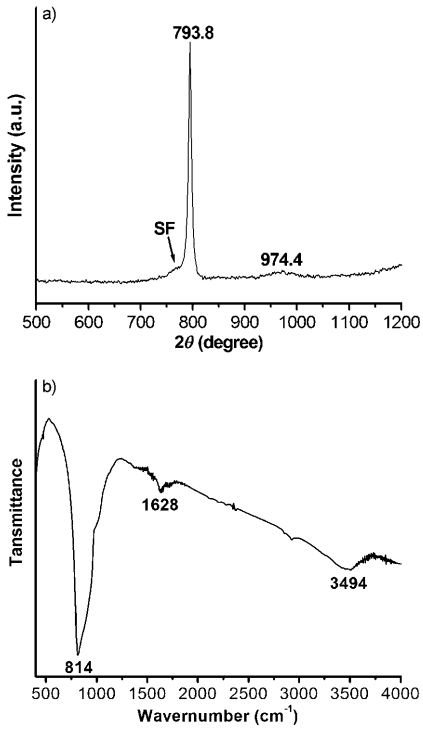


Figure 4. Raman spectrum a) and FTIR spectrum and b) of the ultrathin β-SiC nanowires.

To investigate the formation mechanism of the ultrathin β-SiC nanowires, a series of experiments were carried out, as discussed below. Controlled experiments shown that the products are irregular β-SiC nanoparticles when no 1,10-phenanthroline was added into the reaction system. When 0.1 g 1,10-phenanthroline was added to the reaction system, a large amount of parallel branched β-SiC nanowires with relatively few nanoparticles were obtained (Figure 5). The branched nanowire is composed of a junction and two

  

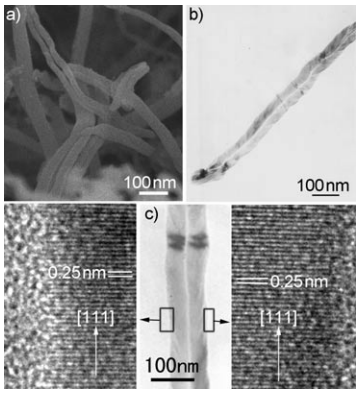


Figure 5. a) FESEM image of the parallel branched β-SiC nanowires. b) TEM image of a parallel branched β-SiC nanowire. c) HRTEM images taken from the edge of a parallel branched β-SiC nanowire.

branches. The branches are approximately parallel along their growth direction, so that we termed them parallel branched β-SiC nanowires. When 0.20 g 1,10-phenanthroline was added in the reaction system, quantities of straight β-SiC nanowires were obtained (Figure 6). The straight β-SiC nanowires are usually 20–40 nm in diameter and 4–10 μm in length. The experimental results suggest that the final morphology of the product is strongly affected by the additive amounts of the 1,10-phenanthroline.

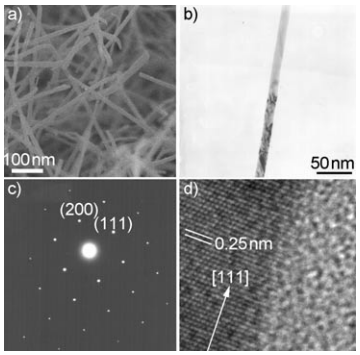


Figure 6. a) FESEM image of the straight β-SiC nanowires. b) TEM image of an individual straight β-SiC nanowire. c) SAED pattern recorded from the β-SiC nanowire. d) HRTEM image taken from the β-SiC nanowire.

Based on the experimental observation, the formation of the ultrathin β-SiC nanowires is rationally proposed to be a 1,10-phenanthroline molecule template mechanism. Figure 7 illustrates the formation process of the ultrathin β-SiC nanowires. As is widely known, 1,10-phenanthroline is a bidentate ligand heterocyclic compound, which can react with many metal ions to form coordination compounds by two N–metal coordinate bonds.[36] One 1,10-phenanthroline molecule contains three aromatic heterocycles, which leads to a

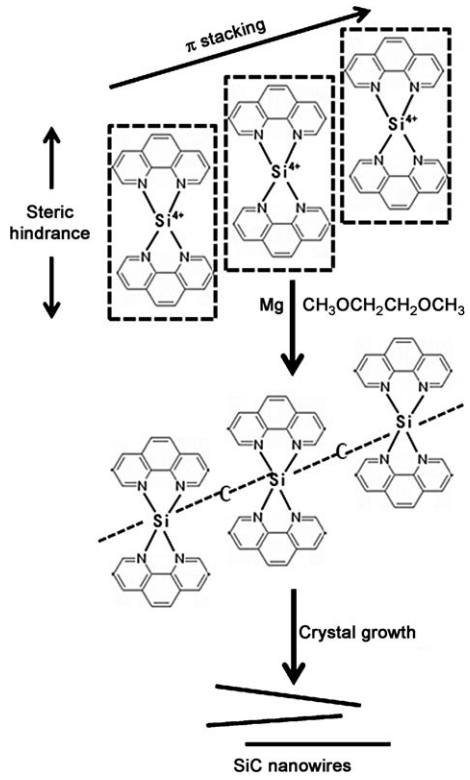


Figure 7. Schematic procedure for the formation mechanism of the ultrathin β-SiC single-crystalline nanowires.

strong steric hindrance effect in these coordination compounds. At the present reaction conditions, two 1,10-phenanthroline molecules react with one $Si^{4+}$ ion to form a coordination compound $[Si–phenanthroline]^{4+}$ by four N–Si coordinated bonds. When the $[Si–phenanthroline]^{4+}$ and the carbon resource $CH_3OCH_2CH_2OCH_3$ contact with the Mg, they will be reduced to Si and C atoms. Then, the Si atoms react with C atoms to generate β-SiC nanocrystals. Obviously, the steric hindrance effect of the coordinated reagent 1,10-phenanthroline on the surface of the Si atoms will result in an oriented growth process to produce β-SiC nanowires along a certain direction. At the same time, the π-stacking induced by the aromatic–aromatic interactions will initiate the linear packing of the $[Si–phenanthroline]^{4+}$ complexes to form a 1D-like assembly. Although this assembly might be very short, consisting of a few $[Si–phenanthroline]^{4+}$ complexes and transient at the present high-temperature reaction system, it still could direct the wire growth. In the present crystal growth process, therefore, 1,10-phenanthroline can be seen as a molecule template that can induce the product to grow into nanowires. When the amount of the 1,10-phenanthroline added in the reaction system is adequate, ultrathin β-SiC nanowires will generate due to the synergistic actions of π-stacking and steric hindrance. On the contrary, when the amount of 1,10-phenanthroline added in the reaction system is insufficient, the π-stacking and steric hindrance effects a not obvious, which can not ef-

  

fectively confine the crystal growth in a certain direction. Therefore, the products are parallel branched nanowires or straight nanowires with larger diameters when the amount of 1,10-phenanthroline is not abundant. The chemical reactions contained in the whole process can be formulated as follows:

$$CH_3OCH_2CH_2OCH_3 + Mg \rightarrow C + MgO + H_2$$

$$SiCl_4 + Mg \rightarrow Si + MgCl_2$$

$$C + Si \rightarrow SiC$$

The photoluminescence (PL) properties of the ultrathin β-SiC nanowires were investigated at room temperature. The PL spectrum of the ultrathin β-SiC nanowires in ethanol solution are shown in Figure 8. A strong green light emission band centered at 500 nm (2.40 eV) is observed. Compared with the band gap of bulk β-SiC at room temperature (2.39 eV), the emission peak position of the ultrathin nanowires is not obviously changed. This observation demonstrates that the emission band of the β-SiC nanowires results from the band-to-band recombination without a quantum confinment effect, which is in good aggrement with the results obtained from β-SiC nanoparticles (6–8 nm).[26] Interestingly, compared with bulk β-SiC, the intensity of the emission peak of the ultrathin nanowires is greatly enhanced. Bulk β-SiC has only a low emission at low-temperature conditions,[37] while strong green light emission of the ultrathin β-SiC nanowires is visible with the naked eye (inset in Figure 8). The enhanced green light emission can be attributed to the very small crystallite size of the ultrathin nanowires.[26] Furthermore, the fluorescence emission intensity of the ultrathin β-SiC nanowires are greater than that of the suspensions of ultrathin β-SiC nanoparticles prepared by catalyzed electrochemical etching of a polycrystalline β-SiC wafer in a HF/ethanol binary solution,[26] which can be attributed to the higher crystallization of the ultrathin nanowires synthesized at realtive higher temperature. In addition, the ultrathin β-SiC nanowires exhibit good solubility in water and ethanol. After ultrasonic treating for 15 min, the suspension of the ultrathin nanowires could stable for 10 days. As a potential fluorescence material, the as-synthesized ultrathin β-SiC nanowires have the advantage over other fluorescence materials in that they have very high mechanical stability, thermal conductivity, and long-term stability to harsh environments. These unique properties suggest that the promising potential of using the as-obtained ultrathin β-SiC nanowires as excellent fluorescence material used under special conditions.

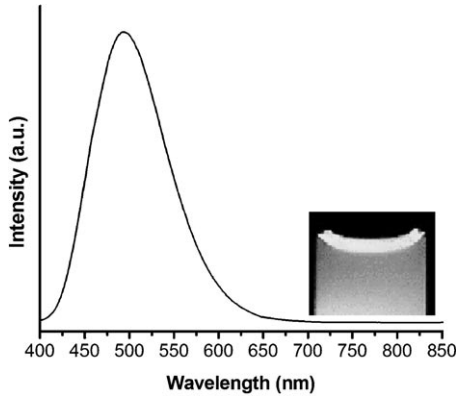


Figure 8. Photoluminescence spectrum of the ultrathin β-SiC nanowires, the insert is the emission photo.

Figure 9 shows the typical current density/electric field ($J/E$) characteristics. Turn-on field ($E_{to}$) and threshold field ($E_{thr}$) are the electric fields required to produce a current

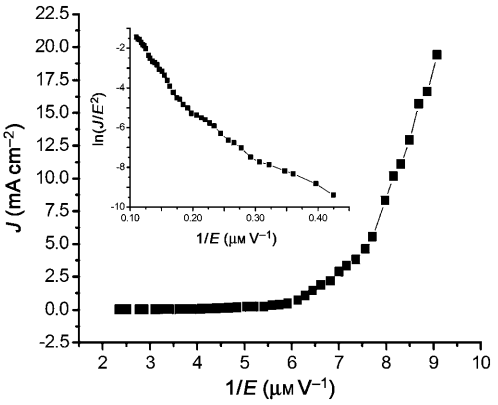


Figure 9. $J/E$ plots of field emission taken from the as-synthesized ultrathin β-SiC nanowires. Insets: the corresponding F–N plot showing approximate linear dependence.

density of 10 μA cm$^{-2}$ and 10 mA cm$^{-2}$, respectively. The $E_{to}$ and $E_{thr}$ of the ultrathin β-SiC nanowires are 3.57 and 8.12 V μm$^{-1}$, and are lower than the $E_{to}$ of β-SiC nanowires (10.5,[38] 10.1,[39] 6.0,[38] 5.0[40] V μm$^{-1}$). The current density is about 20 mA cm$^{-2}$ at 8.9 V μm$^{-1}$, which is greater than the reported 14.6 or 11.5 mA cm$^{-2}$.[41] These data suggest that the ultrathin β-SiC nanowires can be good field emitters. The reason for the low $E_{to}$ and high FE current density can be attributed to their superior structural characteristics, this is, the single-crystalline ultrathin nanowire structure.[42] The behavior of the emission current versus the applied voltage was analyzed using the Fowler–Nordheim equation, $\ln(J/E^2) = -(B\phi^{3/2}/\beta)E^{-1} + \ln(A\alpha\beta^2/\phi)$, where $J$ is the current density, $E$ is the applied field ($V/d$), $\phi$ is the work function, $B$ and $A$ are constants, $\alpha$ is the effective emission area, and $\beta$ is the F–N enhancement factor. The slopes of the corresponding Fowler–Nordheim (F–N) plot shown in the inset of Figure 8 exhibit approximate linear dependence, revealing that the emission currents of the as-sample are caused by the conventional field emission mechanism.

## Conclusion

In summary, a novel ultrathin β-SiC single-crystalline nanowire structure has been prepared through a molecule tem-

  

plate route for the first time. The ultrathin β-SiC nanowires have a single-crystal CZB phase with their axis along the [111] direction, and are about 8 nm in diameter. In this synthetic process, the growth of ultrathin β-SiC nanowires is determined mainly by the strong steric hindrance effect of the 1,10-phenanthroline. By adjusting the amount of 1,10-phenanthroline, parallel branched and straight β-SiC nanowires also can be synthesized in a controlled manner. Stable green light emission at 500 nm was observed in this novel ultrathin β-SiC nanowires and ascribed to the band emission of the CZB phase. FE measurements of the ultrathin β-SiC nanowires show a low turn-on field of 3.57 $V\,\mu m^{-1}$ and a large field-emission current density of 20 $mA\,cm^{-2}$ at 8.9 $V\,\mu m^{-1}$. The excellent field-emission performance is attributed to the specific crystallographic feature with an ultrathin diameter, high aspect ration, and single crystallinity. These results suggest that the ultrathin β-SiC nanowires can be expected to find promising applications as field emitters and optoelectronic devices.

## Experimental Section

**Chemicals**: Silicon tetrachloride ($SiCl_4$), ethylene glycol dimethyl ether ($CH_3OCH_2CH_2OCH_3$), magnesium (Mg), 1,10-phenanthroline ($C_{12}H_8N_2{\cdot}H_2O$), fuming hydrochloride (HCl, 37%), super-pure water (Millipore, 18.2 MΩ cm), absolute ethanol. All reagents used were analytically pure, and were purchased from Beijing Chemical Reagent Company and were used without further purification.

**Preparation of ultrathin β-SiC nanowires**: in a typical synthesis, $SiCl_4$ (3 mL), $CH_3OCH_2CH_2OCH_3$ (0.63 mL), Mg (1.6 g), and moderate amount 1,10-phenanthroline were loaded into a 15 mL stainless steel autoclave. All of the above manipulations were performed in a glove box with flowing nitrogen gas. The autoclave was tightly sealed and heated in an electric stove with an increasing speed of 20 °C $min^{-1}$ and maintained at 650 °C for 6 h, and then cooled down to room temperature naturally. The products in the autoclave can be divided into two parts: gray floccules lay in the top of the autoclave and dark-gray hardy agglomerations deposited on the bottom of the autoclave. The gray floccules were carefully collected and washed with HCl (1 M), distilled water and absolute alcohol, and vacuum-dried at 50 °C for 3 h for characterization.

**Field emission**: The field-emission measurement was carried out in a vacuum chamber with a pressure better than $5\times10^{-6}$ Pa at room temperature under a two-parallel-plate configuration. The as-synthesized products were attached to stainless-steel plate using conducting glue as cathode. Another parallel stainless-steel plate served as the anode at a fix distance of 200 μm during all the measurements. A voltage with a sweep step of 20 V was applied between the anode and cathode to supply an electric field. The emission current was monitored by a Keithley 485 picoammeter.

**Characterization**: XRD pattern of the products was recorded on a Rigaku (Japan) D/max-γA X-ray diffractometer equipped with graphite monochromatized $Cu_{K\alpha1}$ radiation ($\lambda = 1.54178$ Å). The SEM images of the products were examined by a field emission scanning electron microscope (JEOL-6700F). The TEM images, SAED pattern and HRTEM images were recorded on a JEOL 2010 microscope. PL spectrum measurement was performed in a Fluorolog-3-TAU fluorescence spectrophotometer with a Xe lamp at room temperature. FTIR was recorded from a Magna IR-750FT spectrometer. The Raman spectra were produced at room temperature with a LABRAMHR confocal laser micro-Raman spectrometer. The X-ray photoelectron spectrum (XPS) was recorded on a VGESCALAB MKII X-ray photoelectron spectrometer using a non-monochromatized $Mg_{K\alpha}$ X-ray as the excitation source.

## Acknowledgements

We acknowledge the financial support from the Dean Foundation of Chinese Academy of Inspection and Quarantine (2008JK012).

[1] A. P. Alivisatos, *Science* **1996**, *271*, 933.
[2] M. S. Gudiksen, L. J. Lauhon, J. Wang, D. C. Smith, C. M. Lieber, *Nature* **2002**, *415*, 617.
[3] Y. C. Lee, Y. L. Chueh, C. H. Hsieh, M. T. Chang, L. J. Chou, Z. L. Wang, Y. W. Lan, C. D. Chen, H. Kurata, S. Isoda, *Small* **2007**, *3*, 1356.
[4] M. T. Chang, L. J. Chou, C. H. Hsieh, Y. L. Chueh, Z. L. Wang, Y. Murakami, D. Shindo, *Adv. Mater.* **2007**, *19*, 2290.
[5] X. D. Wang, J. H. Song, J. Liu, Z. L. Wang, *Science* **2007**, *316*, 102.
[6] Y. Wu, R. Fan, P. Yang, *Nano Lett.* **2002**, *2*, 83.
[7] Y. Cui, C. M. Lieber, *Science* **2001**, *291*, 851.
[8] L. Manna, E. C. Scher, A. P. Alivisatos, *J. Am. Chem. Soc.* **2000**, *122*, 12700.
[9] E. Braun, Y. Eichen, U. Sivan, G. B. Yoseph, *Nature* **1998**, *391*, 775.
[10] Y. G. Sun, Y. D. Yin, B. T. Mayers, T. Herricks, Y. N. Xia, *Chem. Mater.* **2002**, *14*, 4736.
[11] F. D. Wang, A. G. Dong, J. W. Sun, R. Tang, H. Yu, W. E. Buhro, *Inorg. Chem.* **2006**, *45*, 7511.
[12] T. J. Trentler, K. M. Hickman, S. C. Goel, A. M. Viano, P. C. Gibbons, W. E. Buhro, *Science* **1995**, *270*, 1791.
[13] A. M. Morales, C. M. Lieber, *Science* **1998**, *279*, 208.
[14] R. L. Penn, J. F. Banfield, *Science* **1998**, *281*, 969.
[15] Z. Y. Tang, N. A. Kotov, M. Giersig, *Science* **2002**, *297*, 237.
[16] K. S. Cho, D. V. Talapin, W. Gaschler, C. B. Murray, *J. Am. Chem. Soc.* **2005**, *127*, 7140.
[17] C. Pacholski, A. Kornowski, H. Weller, *Angew. Chem.* **2002**, *114*, 1234; *Angew. Chem. Int. Ed.* **2002**, *41*, 1188.
[18] S. A. Sapp, B. B. Lakshmi, C. R. Martin, *Adv. Mater.* **1999**, *11*, 402.
[19] C. Huber, M. Sadoqi, T. Huber, D. Chacko, *Adv. Mater.* **1995**, *7*, 316.
[20] C. Ma, D. Moore, J. Li, Z. L. Wang, *Adv. Mater.* **2003**, *15*, 228.
[21] Z. W. Pan, Z. R. Dai, Z. L. Wang, *Science* **2001**, *291*, 1947.
[22] X. Lu, D. D. Fanfair, K. P. Johnston, B. A. Korgel, *J. Am. Chem. Soc.* **2005**, *127*, 15718.
[23] Z. Liu, Y. Sakamoto, T. Ohsuna, K. Hiraga, O. Terasaki, C. H. Ko, H. J. Shin, R. Ryoo, *Angew. Chem.* **2000**, *112*, 3237; *Angew. Chem. Int. Ed.* **2000**, *39*, 3107.
[24] V. D. Krstic, *J. Am. Ceram. Soc.* **1992**, *75*, 170.
[25] Z. S. Wu, S. Z. Deng, N. S. Xu, J. Chen, J. Zhou, J. Chen, *Appl. Phys. Lett.* **2002**, *80*, 3829.
[26] X. L. Wu, J. Y. Fan, T, Qiu, X. Yang, G. G. Siu, P. K. Chu, *Phys. Rev. Lett.* **2005**, *94*, 026102.
[27] Z. X. Yang, Y. D. Xia, R. Mokaya, *Chem. Mater.* **2004**, *16*, 3877.
[28] W. Yang, H. Araki, C. Tang, S. Thaveethavorn, A. Kohyama, H. Suzuki, T. Noda, *Adv. Mater.* **2005**, *17*, 1519.
[29] H. Dai, E. W. Wong, Y. Z. Lu, S. S. Fan, C. M. Lieber, *Nature* **1995**, *375*, 769.
[30] T. Seeger, P. K. Redlich, M. Rühle, *Adv. Mater.* **2000**, *12*, 279.
[31] Z. Pan, H. L. Lai, F. C. K. Au, X. Duan, W. Zhou, W. Shi, N. Wang, C. S. Lee, B. Wong, S. T. Lee, S. Xie, *Adv. Mater.* **2000**, *12*, 1186.
[32] G. W. Ho, A. S. W. Wong, A. T. S. Wee, M. E. Welland, *Nano Lett.* **2004**, *4*, 2023.
[33] Z. L. Wang, Z. R. Dai, R. P. Gao, Z. G. Bai, J. L. Gole, *Appl. Phys. Lett.* **2000**, *77*, 3349.
[34] X. H. Sun, C. P. Li, W. K. Wong, N. B. Wong, C. S. Lee, S. T. Lee, B. K. Teo, *J. Am. Chem. Soc.* **2002**, *124*, 14464.
[35] L. S. Liao, X. M. Bao, Z. F. Yang, N. B. Min, *Appl. Phys. Lett.* **1995**, *66*, 2382.
[36] F. P. Dwyer, E. C. Gyarfas, W. P. Rogers, J. H. Koch, *Nature* **1952**, *170*, 190.
[37] M. Ikeda, H. Matsunami, T. Tanaka, *Phys. Rev. B* **1980**, *22*, 2842.
[38] J. J. Niu, J. N. Wang, N. S. Xu, *Solid State Sci.* **2008**, *10*, 618.
[39] G. Z. Shen, Y. Bando, C. H. Ye, B. Liu, D. Golberg, *Nanotechnology* **2006**, *17*, 3468.

  

[40] C. C. Tang, Y. Bando, *Appl. Phys. Lett.* **2003**, *83*, 659.
[41] Z. S. Wu, S. Z. Deng, N. S. Xu, J. Chen, J. Zhou, J. Chen, *Appl. Phys. Lett.* **2002**, *80*, 3829.
[42] X. Fang, Y. Bando, U. K. Gautam, C. Ye, D. Golberg, *J. Mater. Chem.* **2008**, *18*, 509.
[43] X. Fang, Y. Bando, G. Z. Shen, C. Ye, U. K. Gautam, P. M. F. J. Costa, C. Zhi, C. Tang, D. Golberg, *Adv. Mater.* **2007**, *19*, 2593.

Received: September 9, 2009
Revised: November 24, 2009
Published online: March 22, 2010

  